Materials Science-Poland, 35(3), 2017, pp. 626-631
http://www.materialsscience.pwr.wroc.pl/
DOI: 10.1515/msp-2017-0077

DE GRUYTER OPEN

Studies on rheological, structural, optical, electrical and surface properties of $LiMn_2O_4$ thin films by varied spin rates

T. BALAKRISHNAN[1,*], N. SANKARA SUBRAMANIAN[1], A. KATHALINGAM[2]

[1]Thin Film Research Laboratory, Department of Physics, Thiagarajar college of Engineering, Madurai-625015, Tamil Nadu State, India

[2]Millimeter-wave Innovation Technology (MINT) Research Center, Dongguk University, Seoul-04620, South Korea

$LiMn_2O_4$ thin films prepared by cost-effective spin coating method using optimized coating conditions are reported. Spin rate was varied and spin rate dependent properties were studied. Prepared films were characterized for their structural, morphological and optical properties. X-ray diffraction study of $LiMn_2O_4$ thin films confirmed the cubic spinel structure with the preferred orientation along (1 1 1) plane. Optical absorption studies showed band gap energy of 3.02 eV for the grown $LiMn_2O_4$ films. FT-IR bands assigned to asymmetric stretching modes of MnO_6 group were located around 623 cm^{-1} and 514 cm^{-1} for the $LiMn_2O_4$ thin films. The weak band observed at 437 cm^{-1} was attributed to the LiO_4 tetrahedra. The films showed high conductivity value 0.79 S/cm indicating the generation of effective network of the film for enhanced charge transport. AFM micrographs of the $LiMn_2O_4$ films deposited at 3000 rpm and 3500 rpm showed uniform distribution of fine grains throughout the surface without any dark pits, pinholes and cracks.

Keywords: *$LiMn_2O_4$ thin film; sol gel; spin coating, XRD, FT-IR, AFM*

1. Introduction

Spinel lithium manganese oxide ($LiMn_2O_4$) has been extensively studied as the most promising cathode material for lithium-ion batteries, since it is low cost, environmentally friendly, non-toxic, has fast charging-discharging characteristics, good thermal behavior and does not require additional expensive safety device as the layered oxides such as $LiCoO_2$ and $LiNiO_2$ [1, 2].

Nowadays, $LiMn_2O_4$ thin films are fabricated by a variety of methods such as RF magnetron sputtering [3, 4], electrostatic spray deposition [5–8], ultrasonic spray deposition [9], sol-gel spin coating technique [10–18] and so on. The $LiMn_2O_4$ thin films prepared by various methods differ widely in their properties, which is mainly due to the synthesizing procedures. Sol-gel spin coating method is an alternative procedure for the fabrication of $LiMn_2O_4$ thin film cathodes owing to its simplicity as well as economical and easy process. However, the quality of deposited thin films is highly dependent on the nature of precursor solution. The prime requirements of precursor solution are higher order of homogeneity, chemical stability and adherence to substrate surface. Besides, the rate of spin coating also decides of the quality and associated properties of the film. Hence, in this work, we prepared $LiMn_2O_4$ thin films by sol-gel spin coating technique and investigated the influence of spin rate on their structural, optical and surface properties.

2. Experimental

Sol solution was prepared by dissolving lithium acetate ($CH_3COOLi{\cdot}2H_2O$) and manganese nitrate ($Mn(NO_3)_2{\cdot}4H_2O$) in an appropriate amount of ethyl alcohol. Mixed solution was refluxed at 60 °C for about an hour, air cooled and then allowed for aging. Prior to deposition, the substrates were cleaned in double distilled water, then washed in a concentrated chromic acid in order to avoid contamination of the substrate. After that, they were ultrasonically cleaned, finally dried and degreased with acetone. The prepared solution was

*E-mail: baala333@gmail.com

spin coated on the cleaned substrates at various spin rates for 10 s. Ten cycles of spin coating were done; after each spin coating the film was heat treated at 300 °C for 5 min to evaporate the solvents. After the complete cycle of spin coatings, the films were annealed at 400 °C in an atmospheric furnace for 1 hour.

Powder X-ray diffraction (XRD) studies were carried out using Phillips PANanalytical diffractometer with CuKα radiation to measure crystallinity, phases, grain size, microstrain, dislocation density and lattice parameter values for assessing the quality of prepared films. Surface features of the developed thin films were analyzed using an atomic force microscope. Fourier-transform infrared (FT-IR) spectroscopy analysis was carried out on a Shimadzu spectrophotometer to study the configuration of molecular spices and changes in the coordination of the compound. The UV-Vis absorption spectra were recorded using a UV-3101 Shimadzu visible spectrophotometer. Electrical characterization of thin film was carried out using the four probe technique.

3. Results and discussion

3.1. Optimization of spin rate

In spin coating technique, the amount of particles deposited on a substrate depends on the rate of spin. As the film thickness and other properties are varying widely with spin coating rate, optimization of spin rate is important to achieve better properties of the coated thin films. For the deposition, precursor solution was prepared from 1 M lithium acetate and 2 M manganese nitrate dissolved in an appropriate amount of ethyl alcohol. The sol solution was spun onto the glass substrates at different spin rates viz., 2000 rpm, 2500 rpm, 3000 rpm, 3500 rpm and 4000 rpm. The coated films were subjected to heat treatment at 350 °C for 5 min. This procedure was repeated up to 10 times to obtain required layer thickness, and finally the layer was annealed using the atmospheric furnace as mentioned earlier.

3.2. Rheological properties of lithium manganese oxide sol solution

Rheological properties of prepared lithium manganese oxide sol solution were investigated by measuring its density and viscosity for a particular time duration. The prepared alcoholic solution became increasingly cloudy when allowed for aging at room temperature. To analyze the change in viscosity of the solution, its density was measured periodically using Ostwald viscometer. Viscosity was found to increase slowly during the initial period of aging, subsequently, at a stage called break off point, the viscosity increased suddenly to a point called saturation point, and then it stabilized at the same point. This increase in viscosity was due to the occurrence of polymerization, i.e. condensation. The saturation behavior indicated colloidal nature of the gelatinous suspension. Following microscopic changes of the solution during aging period, the break off and saturation point were noted to determine the critical time $t_{1/2.}$ The change in viscosity due to aging is presented in Fig. 1. The critical time $t_{1/2}$ is an ideal time to obtain excellent properties of layers, which was about third day of aging period. Hence, all the lithium manganese oxide thin films were spin coated on the third day of aging.

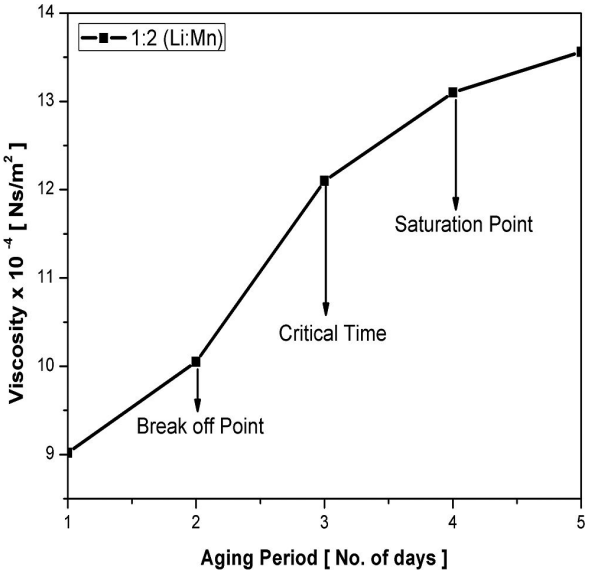

Fig. 1. Effect of solute concentration on the viscosity of sol solution with respect to aging period.

3.3. Structural characterization

X-ray diffraction patterns of $LiMn_2O_4$ thin films deposited at different spin rates viz., 2000 rpm, 2500 rpm, 3000 rpm, 3500 rpm and 4000 rpm in 10 number of coating cycles are shown in Fig. 2. The diffraction peaks of all samples have been identified as typical of cubic spinel structure with space group Fd3m, in which lithium ions occupy tetrahedral (8a) sites and manganese reside at octahedral (16d) sites with preferred orientation along (1 1 1) plane [1]. The other orientations observed in XRD profile correspond to (3 1 1), (4 0 0) and (4 4 0) planes [16, 17]. Sharpness and intensity of all peaks increased with the increase in spin rate indicating crystalline quality improvement at higher spin rates [19–21].

Compared to all spin rates, the 3000 rpm shows highly intense (1 1 1) plane of $LiMn_2O_4$ thin films. It implies that formation of good crystallinity has been achieved at 3000 rpm, which is in good agreement with an earlier report [15]. Lattice constant a evaluated from the XRD data lies between 8.2174 Å and 8.2356 Å, in agreement with standard JCPDS PDF data file number 89-4604.

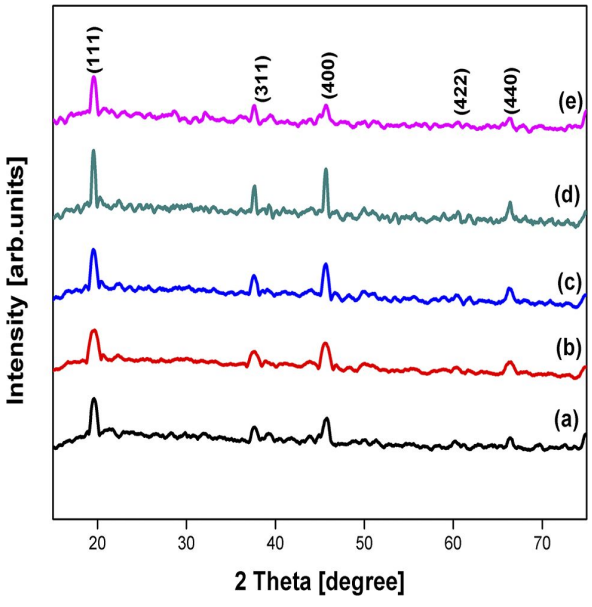

Fig. 2. XRD patterns of $LiMn_2O_4$ thin films spin coated at different spin rates (a) 2000 rpm, (b) 2500 rpm, (c) 3000 rpm, (d) 3500 rpm and (e) 4000 rpm.

Mean crystallite size was calculated using Scherer formula (equation 1) from the XRD data; it is found to vary between 20 nm and 30 nm for the various spin rates as shown in Table 1:

$$D = \frac{0.9\lambda}{\beta \cos\theta} \tag{1}$$

Microstrain and dislocation density were estimated using the relation 2 and relation 3, respectively:

$$\delta = \frac{1}{D^2} \tag{2}$$

$$\varepsilon = \frac{\beta \cos\theta}{4} \tag{3}$$

where D is the crystallite size, β is full width at half maximum.

Crystallite size is indirectly proportional to microstrain. It reveals that higher spin rate resulted in fewer defects in $LiMn_2O_4$ thin films with preferred orientation (1 1 1) [18]. Dislocation density indicates the length of dislocation lines per unit volume and measures the amount of defects in a thin film. The dislocation density and strain are the manifestation of dislocation network in the films, thus a decrease in strain and dislocation density of $LiMn_2O_4$film coated at 3000 rpm indicates formation of higher quality film [19].

3.4. Optical characterization

UV-Vis spectroscopic measurements in the wavelength range 200 to 800 nm were carried out for $LiMn_2O_4$ thin films prepared at spin rates of 3000 rpm and 3500 rpm. Fig. 3a shows the transmittance spectra of the films. They show a gradual decrease of optical transmittance for radiation changing from 310 rpm to 800 nm. The film coated at the spin rate 3000 rpm shows higher transmittance compared to the one spin coated at 3500 rpm.

Absorption coefficient α was calculated from the transmittance spectra using the relation 4 [22], and it is shown in the Fig. 3c:

$$\alpha = 4\pi k_f/\lambda \tag{4}$$

Table 1. Structural parameters of $LiMn_2O_4$ thin films spin coated with different spin rates.

Spin rate [rpm]	Grain size [nm]	Microstrain $\times 10^{14}$ [lines/m^2]	Dislocation density $\times 10^{-3}$ [lines·m^{-4}]	Lattice constant [Å]
2000	21.1	10.7264	5.41	8.2174
2500	24.5	10.2269	5.01	8.2205
3000	27.3	5.9345	5.19	8.2291
3500	32.4	5.0153	3.66	8.2301
4000	29.7	5.3274	4.05	8.2356

where k_f is the extinction coefficient, which can be obtained from the relation 5:

$$k_f = 2.303\lambda \log(1/T_o)/4\pi t \tag{5}$$

where T_o is the transmittance, t is the thickness and λ is the wavelength of the incident radiation.

The plot of the calculated extinction coefficient versus wavelength is shown in Fig. 3b.

Optical band gap of all the films was obtained using the Tauc relation 6 [23]:

$$\alpha h\upsilon = A(h\upsilon - E_g)^{1/2} \tag{6}$$

where α is the optical absorption coefficient near the fundamental absorption edge, hυ is the photon energy and A is a constant. As can be seen in Fig. 3d, the plots of $(\alpha h\upsilon)^2$ versus hυ are mostly linear over a wide range of photon energies, indicating the direct type of transition. Hence, the band gap values were estimated by extrapolating the curves across the x-axis at the onset of absorption. The intercepts (extrapolations) of these plots (straight lines) on the energy axis $[(\alpha h\upsilon)^2 = 0]$ give the energy band gap values [24]. The band gap values are 2.97 eV and 3.02 eV for the films deposited at the spin rates 3500 and 3000 rpm, respectively, with an accuracy of ±0.04 eV [25].

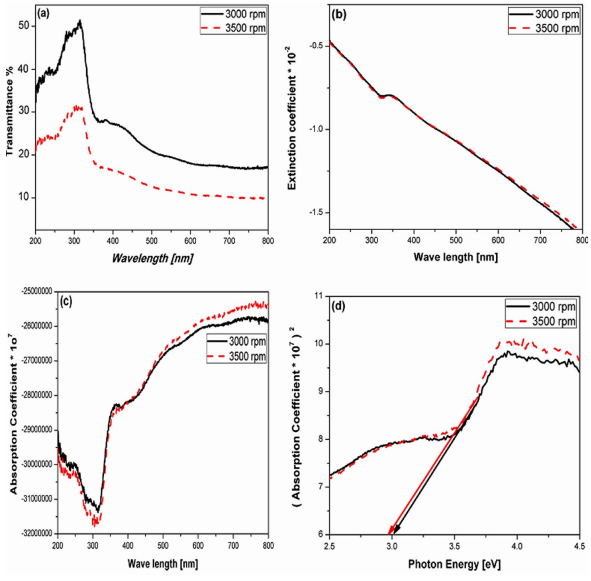

Fig. 3. Results of optical studies on $LiMn_2O_4$ thin films (a) optical transmittance spectra (b) variation of extinction coefficient with wavelength (c) variation of absorption coefficient with wavelength (d) plots of $(\alpha h\upsilon)^2$ vs. photon of energy (hυ).

3.5. FT-IR analysis

FT-IR spectra observed for $LiMn_2O_4$ thin films coated at different spin rates are shown in Fig. 4. Three vibrational modes around 437 cm^{-1}, 514 cm^{-1} and 623 cm^{-1} are observed for all the films. The two higher wave number peaks could be assigned to asymmetric stretching vibration of Mn–O_6 group and the lower wave number peak corresponds to tetrahedral stretching vibration of Li–O_4 group, and these results are in a good agreement with reported results [26].

3.6. Electrical studies

Electrical conductivity of the films was measured at room temperature by a standard four-probe method, using Keithley 2180 nanovoltmeter and Keithley 2400 source meter. The measured electrical conductivity values of $LiMn_2O_4$ thin films for different spin rates are summarized in Table 2, and they are found to strongly depend on spin rate. The $LiMn_2O_4$ thin film prepared at 3000 rpm shows

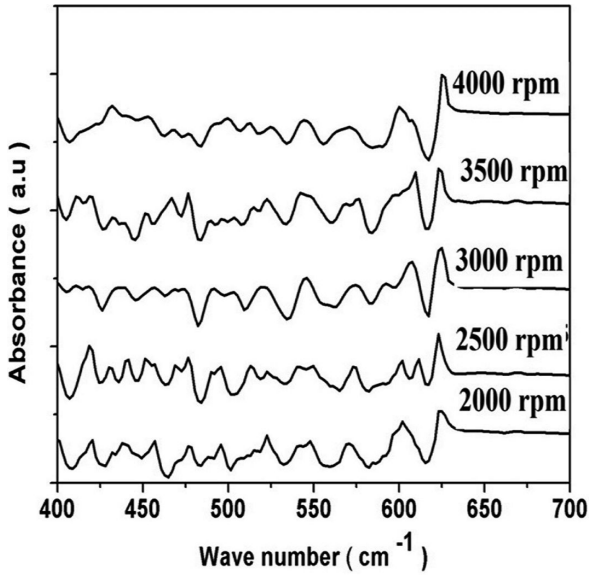

Fig. 4. FT-IR spectra of $LiMn_2O_4$ thin films spin coated at different spin rates.

the largest conductivity value of 0.87 S/cm compared to other films. The highest conductivity of the film coated at 3000 rpm results probably from the generation of more effective network for charge transport.

Table 2. Electrical conductivity of $LiMn_2O_4$ thin films spin coated at different spin rates.

Sample [rpm]	Conductivity [S/cm]
2000	0.81
2500	0.85
3000	0.87
3500	0.86
4000	0.79

3.7. Surface morphological characterization

Fig. 5 shows the SEM images of $LiMn_2O_4$ thin films coated at various spin rates. The film coated at 2000 rpm shows cracked nature, it seems that the higher thickness is connected with low spin rate. At higher spin rate, the film shows very rough surface with grains of various sizes. The film grown at 3000 rpm seems to be better than the films grown at other spin rates.

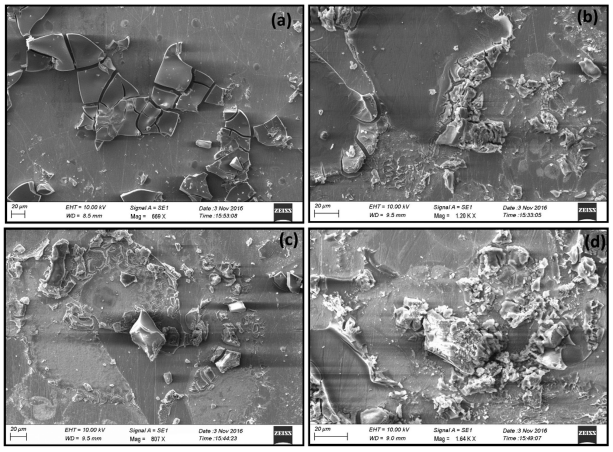

Fig. 5. SEM images of $LiMn_2O_4$ thin films spin coated at spin rates (a) 2000 rpm, (b) 2500 rpm, 3000 rpm and 3500 rpm.

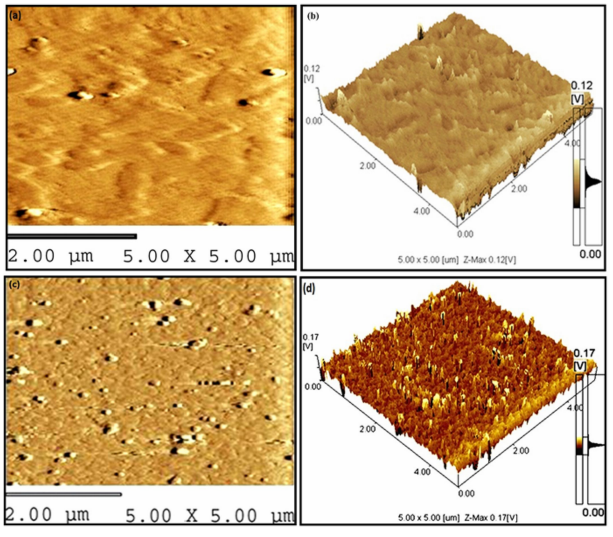

Fig. 6. 2D and 3D AFM images of $LiMn_2O_4$ thin films spin coated at 3000 rpm (a and b), and 3500 rpm (c and d).

AFM surface analysis was done for the films deposited at 3000 rpm and 3500 rpm, and the results are shown in the Fig. 6. They show 2D and 3D AFM images of $LiMn_2O_4$ thin films. The film coated at 3000 rpm has uniform surface with large and coarse grains distributed unevenly on the substrate. The bigger grains are the agglomeration of smaller particles. No cracks or pinholes are observed in the films coated above 3000 rpm [5].

4. Conclusions

$LiMn_2O_4$ thin films were successfully coated using cost effective spin coating method at different spin rates. XRD results confirmed the formation of $LiMn_2O_4$ films of cubic spinel structure with preferred orientation along (1 1 1) plane. The films coated at 3000 rpm showed improved crystalline structure with higher peak intensity and sharpness. They also revealed an increase in accumulation and adhesion of crystallites as well as decreased microstrain and dislocation density. Lattice constant a evaluated from XRD data was between 8.2174 Å and 8.2356 Å. The band gap value of the films grown at 3000 rpm spin rate was about 3.02 eV. FT-IR spectra of $LiMn_2O_4$ thin films confirmed stretching and vibration bands of $LiMn_2O_4$. AFM micrographs of $LiMn_2O_4$ films coated at 3000 rpm indicated smooth deposition with uniform distribution of fine grains throughout the surface.

References

[1] TANIGUCHI I., FUKUDA N., KONAROVA M., *Adv. Powder Technol.*, 181 (2008), 228.

[2] YANG L., TAKAHASHI M., WANG B., *Electrochim. Acta*, 51 (2006), 3228.

[3] CHEN C.C., CHIU K.-F., LIN K.M., LIN H.C., *Thin Solid Film*, 517 (2009), 4192.

[4] MOON H.-S., LEE W., REUCROFT P.J., PARK J.-W., *J. Power Sources*, 119 – 121 (2003), 710.

[5] DOI T., YAHIRO T., OKADA S., *Electrochim. Acta*, 53 (2008), 8604.

[6] CHEN C.H., KELDER E.M., SCHOONMAN J., *J. Power Sources*, 68 (1997), 377.

[7] SUBRAMANIA A., KARTHICK S.N., ANGAYARKANNI N., *Thin Solid Films*, 516 (2008), 8295.

[8] IRIYAMA Y., TACHIBANA Y., SASASOKA R., KUWATA N., ABE T., INABA M., TASAKA A., KIKUCHI K., KAWAMURA J., OGUMI Z., *J. Power Sources*, 174 (2007), 1057.

[9] WANG Y., CHEN W., LUO Q., XIE S., CHEN C.H., *Appl. Surf. Sci.*, 252 (2006), 8096.

[10] TIAN L., YUAN A., *J. Power Sources*, 192 (2009), 693.

[11] TAN C.L., ZHO U., LI W.S., HOU X.H., LU D.S., XU M.Q., HUNG Q.M., *J. Power Sources*, 184 (2008) 408.

[12] PARK Y.J., KIM J.G., KIM M.K., CHUNG H.T., PARK Y., *J. Power Sources*, 87 (2000), 69.

[13] JANG S.-W., LEE H.-Y., SHIN K.-C., LEE S.M., LEE J.-K., LEE S.-J., BAIK H.-K., RHEE D.-S., *J. Power Sources*, 88 (2000), 274.

[14] SUN Y.-K., *Solid State Ionics*, 100 (1997), 115.

[15] LIANG H., ZHAO X., YU Z., CAO M., LIU H., *Solid State Ionics*, 192 (2011), 339.

[16] SHIH F.-Y., FUNG K.-Z., *J. Power Sources*, 159 (2006), 179.

[17] SHIH F.-Y., FUNG K.-Z., *J. Power Sources*, 158 (2006), 1370.

[18] CHIU K.F., LIN H.C., LIN K.M., CHEN C.C., *J. Electrochem. Soc.*, 153 (10) (2006), 1992.

[19] KHATUN F., GAFU M.A., ALI M.S., ISLAM M.S., SARKER A.R., *J. Sci. Res.*, 6 (2) (2014), 217.

[20] TSUJI T., NAGAO M., YAMAMURA Y., TAI N.T., *Solid State Ionics*, 154 – 155 (2002), 381.

[21] BJORK H., GUSTAFSSON T., THOMAS J.O., *Electrochemistry*, 3 (2001), 187.

[22] SARMA P.H., SUBRAMANIAN V., RANGARAJAN N., MURALI K.R., *Bull. Mater. Sci.*, 18 (1995), 875.

[23] TANEMURA S., MIAO S., JIN P., KANEKO K., TERAI A., NABATOVA-GABAIN N., *Appl. Surf. Sci.*, 654 (2003), 654.

[24] BOUWMAN P.J., BOUKAMP B.A., BOUWMEESTER H.J.M., RAMANA C.V., *Solid State Ioninics*, 152 (2002), 181.

[25] NOURI J., KHOSHRAVESH T., KHANAHMADZADEH S., SALEHABADI A., ENHESSARI M., *Int. J. Nano Dimens.*, 7 (1) (2016), 15.

[26] KALYANI P., KALAISELVI N., MUNIYANDI N., *J. Power Sources*, 111 (2002), 232.

Received 2017-03-02
Accepted 2017-09-02